AN INVESTIGATION ON MAGNETIC CHARACTERISTICS OF RING MAGNET FOR WHEELED IN-PIPE AND OUT-PIPE ROBOTS

RAJENDRAN SUGIN ELANKAVI, D. DINAKARAN, R.M. KUPPAN CHETTY, M.M. RAMYA and JAISE JOSE

Centre for Automation and Robotics (ANRO), School of Mechanical Sciences, Hindustan Institute of Technology and Science, Chennai, Tamil Nadu, India.
E-mail: rs.ser0819@hindustanuniv.ac.in, dinakaran@hindustanuniv.ac.in, kuppanc@hindustanuniv.ac.in, mmramya@hindustanuniv.ac.in and rs.jj1217@hindustanuniv.ac.in

The magnetic adhesion of ring magnets classified under permanent magnets, which are employed in magnetic wheels for In-Pipe and Out-Pipe robots, is investigated in this paper. The study is carried out using FEMM software for ring magnets by changing their inner diameter and thickness against a minimum pipeline thickness. The results show that the adhesion force increases as the magnet thickness increases and reduces as the magnet's inner diameter increases. When it comes to inner and outer pipelines, the positioning of ring magnets is also a challenge. This is demonstrated using solidworks software by modelling a ring magnet and laying it over the inner and outer pipelines. Ring magnets of various thicknesses were found to be necessary for diverse pipeline diameters. So based on FEMM simulation and visualization from solidworks the optimal thickness and inner diameter for the ring magnet are derived. The simulation results help researchers choose the optimal ring magnet for the magnetic wheel for both In-Pipe and Out-Pipe robots.

Keywords: Wheel, Magnetic Adhesion, Permanent Magnets, Inspection robot, Pipeline robot, Mobile robot

1. Introduction

Pipelines are used in industries to transport fluids, liquids, and gases. They are also one of the most efficient methods, but they must be monitored on a regular basis to function properly. Since humans are unable to enter small pipes and it is dangerous for them to inspect pipelines at great heights, robotic-based inspection was developed. The pipeline inspection robots are classified into two types: In-Pipe Inspection Robots [1], [2] and Out-Pipe Inspection Robots [3], [4]. Out-Pipe robots are preferred over In-Pipe robots because they do not require the pipeline to be shut down during inspection [5]. In industries, inspecting pipelines at high altitudes is difficult, necessitating the use of robots capable of climbing vertical pipes. The adhesion systems used for climbing vertical pipes are divided into five types [6], [7]. It consists of biometric [8]–[11], vacuum suction[12], rail-guided[13]–[15], gripping [16], [17] and magnetic adhesion[18].

The biometric adhesion mimics geckos and gives the required stickiness to climb [19], [20]. Suction cups are used in vacuum suction to create a pressure difference, which provides the necessary adhesion force to climb the surface. This is not limited to a single surface, but can be extended to a variety of surfaces such as glass, tiles, and steel [21]. Rails are used in rail-guided adhesion to give the necessary traction for climbing vertically. The robot follows the path of the rails and slide over it [13], [14]. Places that require force monitoring uses gripping mechanism and this provides the necessary adhesion to move in uneven surfaces and sophisticated environments [16], [17].

Ferromagnetic pipes are used in industry to transfer liquids and gases [22]. As a result, a robot capable of moving across ferromagnetic surfaces is required. Hence, robot uses magnetic adhesion of permanent magnets to move vertically and the magnets are used as tracks, wheels and in some they are attached to the body. The magnetic adhesion provides high payload capability, safer even during power failure with zero power consumption. The wheeled magnetic adhesion is best suited since magnets attached to the robot causes stress on its body [23].

The focus of this work is solely on wheeled magnetic adhesion based on permanent magnets. The wheels climb vertically on ferrous surfaces by using a permanent magnet and its adhesion. The variation of adhesion for ring magnets is investigated by varying their inner diameter and thickness. The Finite Element Method for Magnetics (FEMM) software is used to simulate the study. The results from simulation assists researchers in selecting the optimal ring magnet for the robot wheel, which is utilised to move in the inner and outer ferromagnetic pipes.

2. Materials Used

In this study Neodymium ring magnets are used to provide the necessary magnetic adhesion to climb vertical pipes. The wheel holds the ring magnet which acts as the adhesion module. The magnetic wheel is shown in figure 1.
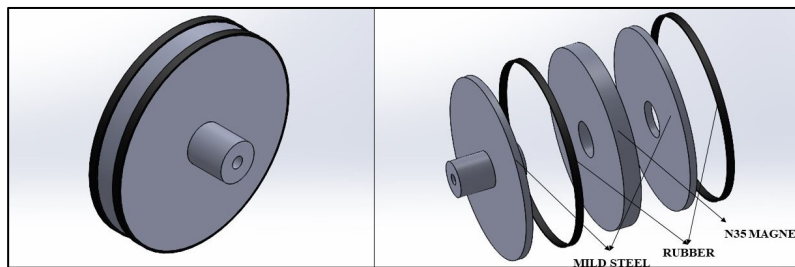

Figure 1. Magnetic wheel

2.1. *Permanent magnet*

The simulation uses ring magnet that come under the classifications of neodymium magnets. These are one of the most powerful permanent magnets and their name starts with 'N' followed by two numbers. 'N' stands for Neodymium and the two numbers show the maximum energy product in Mega-Gauss Oersteds (MGOe). The commercially available magnets range from N30 to N52. In this simulation, a N35 magnet is utilised, and the material properties are extracted from the FEMM software's built-in library. Table 1 shows the properties of N35 magnet.

Table 1. Properties of N35 magnet [18]

Grade of Magnets	Energy product of the magnet BH max, MGOe	Remanent magnetization Br, T	Coercive force HcB, KA/m	Electric Conductivity γ, MS/m
N35	34	1.2	905	0

2.2. *Ferromagnetic surface*

The simulation uses 1020 steel for the surface. This comes under the category of low carbon steel and these are widely used in industries. It is seen from studies [18] [24] that surface thickness has a significant impact on magnetic adhesion, and magnetic adhesion increases as surface thickness increases. So, in this simulation, the pipeline surface thickness is maintained to a minimum so that we may determine the maximum magnet adhesion force generated by the magnet for an extremely low surface thickness. Table 2 shows the properties of 1020 steel.

Table 2. Properties of 1020 steel [18]

Saturation flux density Bsat	NaN
Coercivity Hc, A/m	0
Relative permeability μ	760
Electric conductivity γ, [MS/m]	5.8

3. Simulation using FEMM

The FEMM software is used to simulate the magnetic adhesion of ring magnets [25] [26]. As this is a 2D software, the pipe and ring magnet are drawn in 2D as well. Since the magnet cannot come into direct contact with the surface, it is kept at a minimum standoff distance (SOD) of 0.5mm. The simulation is divided into three stages: pre-processing – processing – post-processing [25]. The problem is characterised as magnetostatics in the first stage, and the depth is given for both the ring magnet and the surface, along with the units. The 2D diagram of the ring magnet and pipe is then created using the built-in tools. The built-in library is then used to specify the material attributes for the components. The entire model is then encased in a circle, which serves as the boundary. Figure 2 shows the entire model with assigned materials in FEMM. In the second stage, the software meshes the entire model using the triangle meshing process, and the analysis is done. In the final stage, the findings are viewed, and the flux density and magnetic adhesion force are calculated using the tools. This process is then repeated by changing the internal diameter and thickness of the ring magnet.
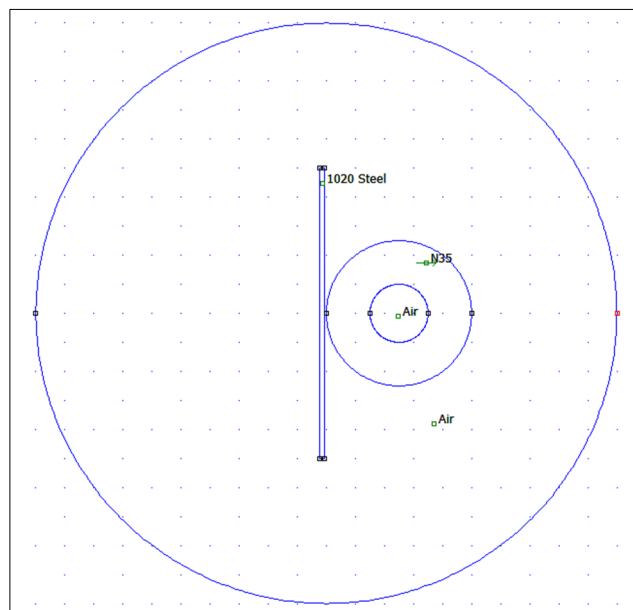

Figure 2. Entire model with assigned materials in FEMM

4. Results and Discussions

The simulation is performed to determine the magnetic adhesion of ring magnets used as wheels. This study is for robots that employ magnetic wheels in ferromagnetic pipes, both within and outside the pipe. The simulation study shows the magnetic adhesion of three different inner diameter and thickness ring magnets. The adhesion generated by the ring magnets is shown in table 3. The outside diameter of the ring magnet is 50 mm, and it is set at a SOD of 0.5 mm from the pipe surface, with a thickness of 2 mm, both of which remain constant during the simulations.

Table 3. FEMM simulation results for magnetic adhesion of ring magnets

Varying Inner Diameter (ID) of ring magnet (mm)	Thickness of ring magnet (mm)	Force Experienced by Pipe surface in Newton (N)
10	5	20.91
10	10	41.82
10	15	62.72
20	5	17.86
20	10	35.73
20	15	53.59
30	5	12.85
30	10	25.69
30	15	38.54

The simulation results show that the adhesion force increases as the thickness of the ring magnet increases for all internal diameters of the ring magnet. A ring magnet with a high thickness and a small internal diameter achieves the maximum adhesion force of 62.72 N. Figure 3 shows the graphical represents of Table 3 data.
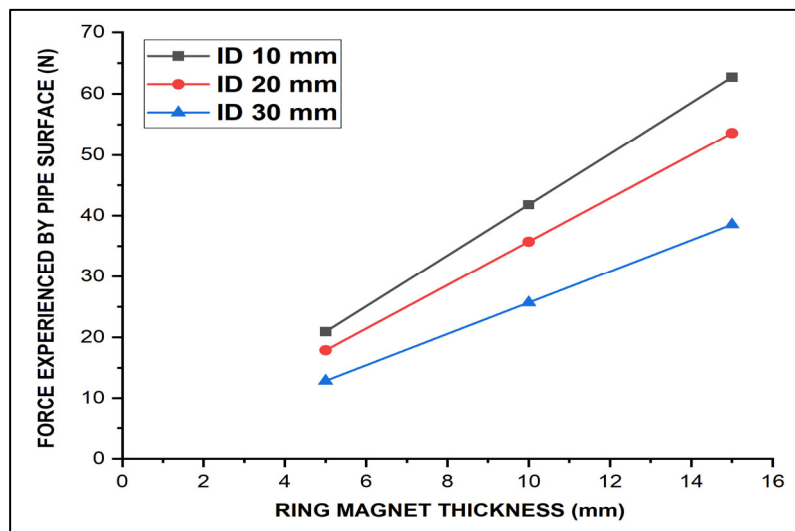

Figure 3. Graphical representation of table 3 data

While selecting ring magnet for the wheels the optimal thickness must be known because the wheels will be in contact with the convex (Out-Pipe) and concave (In-Pipe) part of the pipe. This is tested by modelling a ring magnet and placing it on a modelled In-Pipe and Out-Pipe

using solidworks. When the wheels are in contact with the convex part of the pipe the bigger the thickness of the magnet the weight of the magnet increases and as the pipe surface is convex the edges of the magnet will not be in contact. When the wheels are in contact with the concave part of the pipe only the edges of the magnet will be in contact. So, the point of contact differs for both Out-Pipe and In-Pipe. Thus, the excess thickness causes the magnet to create a natural standoff distance in the case of In-Pipe and in the case of Out-Pipe the excess thickness is bigger than the contact area of the surface. The contact area of magnet for both Out-Pipe and In-Pipe is shown in table 4.

Table 4. Contact area of ring magnet for both Out-Pipe and In-Pipe

Pipeline Diameter	Magnet Thickness	Out-Pipe	In-Pipe
Outer: 50 mm Inner: 46 mm	5 mm		
	10 mm		
	15 mm		

Table 4 shows that increasing the thickness of the magnet causes a standoff distance from the surface at the centre of the magnet for the In-Pipe and at the magnet's edges for the Out-Pipe. This shows that the robot requires magnetic wheels of variable thicknesses to move over In-Pipe and Out-Pipe of varying diameters. So, to lower the weight of the magnetic wheel while maintaining a constant thickness for the magnet, a ring magnet with a thickness of 5 mm and an inner diameter of 10 mm is chosen as a constant that can manuver across inner and outer pipelines with diameters larger than 50 mm. This configuration of magnet has an adhesion force of 20.91 N when kept at a standoff distance of 0.5 mm from the surface.

5. Conclusion

In this research, the influence of ring magnet inner diameter and thickness on magnetic adhesion of Neodymium magnets is investigated using simulations. FEMM software is used to find the adhesion force generated by N35 ring magnet. For ring magnets, the simulation is carried out by varying the inner diameter and thickness while maintaining the outer diameter at 50 mm, pipe surface thickness at 2 mm and standoff distance at 0.5 mm. The results show that the adhesion force increases when the thickness of the magnet increases and decreases when the inner diameter of the magnet increases.

Solidworks is used to model a ring magnet and place it on the inner and outer pipe to find the optimal ring magnet. It is found that for the In-Pipe the edges of magnet will be in contact with the pipe surface while for the Out-Pipe the edges of the magnet will not be in contact and this creates a natural standoff distance. The higher the standoff distance lower will be adhesion force.

So, for varying pipeline diameter, ring magnets of different thickness needs to be used. Hence, an optimal ring magnet which can be used to manuver over outer and inner pipeline having lesser weight with a constant thickness is selected from the simulation results. The optimal ring magnet found has an inner diameter of 10mm, outer diameter of 50 mm, thickness of 5 mm and this configuration has an adhesion force of 20.91 N when kept at a standoff distance of 0.5 mm from the surface. The work done is limited to simulation and this can further be verified using experiments.

References

1. Li, H., Li, R., Zhang, J., & Zhang, P. (2020). Development of a pipeline inspection robot for the standard oil pipeline of china national petroleum corporation. *Applied Sciences (Switzerland)*, *10*(8). https://doi.org/10.3390/APP10082853
2. Elankavi, R. S., Dinakaran, D., & Jose, J. (2020). Developments in Inpipe Inspectionrobot: a Review. *Journal of Mechanics of Continua and Mathematical Sciences*, *15*(5). https://doi.org/10.26782/jmcms.2020.05.00022
3. Sarvestani, A. A., Eghtesad, M., Fazlollahi, F., Goshtasbi, A., & Mokhtari, K. (2016). Dynamic modeling of an out-pipe inspection robot and experimental validation of the proposed model using image processing technique. *Iranian Journal of Science and Technology - Transactions of Mechanical Engineering*, *40*(1). https://doi.org/10.1007/s40997-016-0012-x
4. Choi, C., Park, B., & Jung, S. (2010). The design and analysis of a feeder pipe inspection robot with an automatic pipe tracking system. *IEEE/ASME Transactions on Mechatronics*, *15*(5). https://doi.org/10.1109/TMECH.2009.2032541
5. Ali, M. H., Zharakhmet, T., Atykhan, M., Yerbolat, A., & Batai, S. (2018). Development of a robot for boiler tube inspection. *ICINCO 2018 - Proceedings of the 15th International Conference on Informatics in Control, Automation and Robotics*, *2*(Icinco), 534–541. https://doi.org/10.5220/0006930205340541
6. Nansai, S., & Mohan, R. E. (2016). A survey of wall climbing robots: Recent advances and challenges. *Robotics*, *5*(3), 1–14. https://doi.org/10.3390/robotics5030014
7. Chu, B., Jung, K., Han, C. S., & Hong, D. (2010). A survey of climbing robots: Locomotion and adhesion. *International Journal of Precision Engineering and Manufacturing*, *11*(4), 633–647. https://doi.org/10.1007/s12541-010-0075-3
8. Hou, X., Su, Y., Jiang, S., Cao, P., Xue, P., Tang, T., Li, L., & Chen, T. (2019). Space climbing robot feet with microarray structure based on discrete element method. *International Journal of Robotics and Automation*, *34*(1). https://doi.org/10.2316/J.2019.206-5096
9. Chattopadhyay, P., & Ghoshal, S. K. (2018). Adhesion technologies of bio-inspired climbing robots: A survey. *International Journal of Robotics and Automation*, *33*(6). https://doi.org/10.2316/Journal.206.2018.6.206-5193
10. Menon, C., & Sitti, M. (2005). Biologically inspired adhesion based surface climbing robots. *Proceedings - IEEE International Conference on Robotics and Automation*, *2005*(April), 2715–2720. https://doi.org/10.1109/ROBOT.2005.1570524
11. Carlo, M., & Metin, S. (2006). A Biomimetic Climbing Robot Based on the Gecko. *Journal of Bionic Engineering*, *3*(3), 115–125. https://doi.org/10.1016/S1672-6529(06)60015-2
12. Brusell, A., Andrikopoulos, G., & Nikolakopoulos, G. (2016). A survey on pneumatic wall-climbing robots for inspection. *24th Mediterranean Conference on Control and Automation, MED 2016*, 220–225. https://doi.org/10.1109/MED.2016.7535885
13. Warszawski, A. (2003). Industrialized and automated building systems: A managerial approach. In *Industrialized and Automated Building Systems: A Managerial Approach*. https://doi.org/10.4324/9780203223697
14. Bach, F. W., Rachkov, M., Seevers, J., & Hahn, M. (1995). High tractive power wall-

climbing robot. *Automation in Construction*, *4*(3). https://doi.org/10.1016/0926-5805(95)00005-L

15. Elkmann, N., Felsch, T., Sack, M., Saenz, J., & Hortig, J. (2002). Innovative service robot systems for facade cleaning of difficult-to-access areas. *IEEE International Conference on Intelligent Robots and Systems*, *1*. https://doi.org/10.1109/IRDS.2002.1041481

16. Balaguer, C., Gimenez, A., & Abderrahim, M. (2002). ROMA robots for inspection of steel based infrastructures. *Industrial Robot*, *29*(3). https://doi.org/10.1108/01439910210425540

17. Krosuri, S. P., & Minor, M. A. (2003). A multifunctional hybrid hip joint for improved adaptability in miniature climbing robots. *Proceedings - IEEE International Conference on Robotics and Automation*, *1*. https://doi.org/10.1109/robot.2003.1241614

18. Jose, J., Devaraj, D., Mathanagopal, R. M., Ramanathan, K. C., Tokhi, M. O., & Sattar, T. P. (2021). Investigations on the effect of wall thickness on magnetic adhesion for wall climbing robots. *International Journal of Robotics and Automation*, *36*(3). https://doi.org/10.2316/J.2021.206-0441

19. Yu, Z., Shi, Y., Xie, J., Yang, S. X., & Dai, Z. (2018). Design and analysis of a bionic adhesive foot for gecko robot climbing the ceiling. *International Journal of Robotics and Automation*, *33*(4). https://doi.org/10.2316/Journal.206.2018.4.206-5412

20. Yu, Z., Yang, B., Yang, S. X., & Dai, Z. (2017). Vertical climbing locomotion of a new gecko robot using dry adhesive material. *International Journal of Robotics and Automation*, *32*(4). https://doi.org/10.2316/Journal.206.2017.4.206-5054

21. Fanni, M. A., Alkalla, M. G., & Mohamed, A. (2018). Propeller-type skid steering climbing robot based on a hybrid actuation system. *International Journal of Robotics and Automation*, *33*(3). https://doi.org/10.2316/Journal.206.2018.3.206-5017

22. Lai, S., Chen, D. Y., Chen, H., & Fu, Y. W. (2015). Pulsed Eddy Current Testing of Inner Wall Flaws in Pipe under Insulation. *Procedia Engineering*, *130*. https://doi.org/10.1016/j.proeng.2015.12.334

23. Jose, J., Sugin Elankavi, R., Dinakaran, D., Kuppan Chetty, R. M., & Ramya, M. M. (2021). A Comparative Study of Adhesion Mechanism for Wall Climbing Robots: Ring Magnet vs. Block Magnets. *IOP Conference Series: Materials Science and Engineering*, *1145*(1), 012063. https://doi.org/10.1088/1757-899x/1145/1/012063

24. Wang, R., & Kawamura, Y. (2016). An Automated Sensing System for Steel Bridge Inspection Using GMR Sensor Array and Magnetic Wheels of Climbing Robot. *Journal of Sensors*, *2016*. https://doi.org/10.1155/2016/8121678

25. Meeker, D. (2019). Finite Element Method Magnetics: HomePage. *Femm.Info*.

26. Baltzis, K. B. (2008). The FEMM package: A simple, fast, and accurate open source electromagnetic tool in science and engineering. *Journal of Engineering Science and Technology Review*, *1*(1). https://doi.org/10.25103/jestr.011.18